DR. YAPING CHEN (Orcid ID : 0000-0003-1372-8861)

Article type : Primary Research Articles

Divergent shrub-cover responses driven by climate, wildfire, and permafrost interactions in Arctic tundra ecosystems

Yaping Chen[1], Feng Sheng Hu[1,2,3,4], Mark J. Lara[1,5]

[1]Department of Plant Biology, University of Illinois at Urbana-Champaign, Illinois, USA

[2]Department of Geology, University of Illinois at Urbana-Champaign, Illinois, USA

[3]Department of Biology, Washington University in Saint Louis, Missouri, USA

[4]Department of Earth and Planetary Sciences, Washington University in Saint Louis, Missouri, USA

[5]Department of Geography, University of Illinois at Urbana-Champaign, Illinois, USA

Corresponding authors:

Feng Sheng Hu (fshu@wustl.edu; 217.244.2082)

Mark J. Lara (mjlara@illinois.edu; 915.240.4277)

Running title

Fire-shrub interactions vary across space

Abstract

The expansion of shrubs across the Arctic tundra may fundamentally modify land-atmosphere interactions. However, it remains unclear how shrub expansion pattern is linked with key environmental drivers, such as climate change and fire disturbance. Here we used 40+ years of high-resolution (~1.0 m) aerial and satellite imagery to estimate shrub-cover change in 114 study sites

This article has been accepted for publication and undergone full peer review but has not been through the copyediting, typesetting, pagination and proofreading process, which may lead to differences between this version and the Version of Record. Please cite this article as doi: 10.1111/GCB.15451

across four burned and unburned upland (ice-poor) and lowland (ice-rich) tundra ecosystems in northern Alaska. Validated with data from four additional upland and lowland tundra fires, our results reveal that summer precipitation was the most important climatic driver (r = 0.67, p < 0.001), responsible for 30.8% of shrub expansion in the upland tundra between 1971 and 2016. Shrub expansion in the uplands was largely enhanced by wildfire (p < 0.001) and it exhibited positive correlation with fire severity (r = 0.83, p < 0.001). Three decades after fire disturbance, the upland shrub cover increased by 1077.2 ± 83.6 m^2 ha^{-1}, ~7 times the amount identified in adjacent unburned upland tundra (155.1 ± 55.4 m^2 ha^{-1}). In contrast, shrub cover markedly decreased in lowland tundra after fire disturbance, which triggered thermokarst-associated water impounding and resulted in 52.4% loss of shrub cover over three decades. No correlation was found between lowland shrub cover with fire severity (r = 0.01). Mean summer air temperature (MSAT) was the principal factor driving lowland shrub-cover dynamics between 1951 and 2007. Warmer MSAT facilitated shrub expansion in unburned lowlands (r = 0.78, p < 0.001), but accelerated shrub-cover losses in burned lowlands (r = –0.82, p < 0.001). These results highlight divergent pathways of shrub-cover responses to fire disturbance and climate change, depending on near-surface permafrost and drainage conditions. Our study offers new insights into the land-atmosphere interactions as climate warming and burning intensify in high latitudes.

Keywords

Arctic tundra; Climate change; Permafrost degradation; Shrub expansion; Thermokarst; Drainage; Wildfire disturbance

1. INTRODUCTION

Air temperature in the Arctic has risen at a rate of 0.5 °C per decade since 1980s, nearly doubling that of the global average (Serreze & Barry 2011). In response to amplified Arctic warming, growing evidence points to increases in the frequency, magnitude, and severity of tundra fires (Mack et al. 2011; Hu et al. 2015; Michaelides et al. 2019). These fire-regime changes in turn strongly influence vegetation composition, surface energy dynamics, and nutrient cycling (Mack et al. 2011; Lantz et al. 2010; Rocha et al. 2012; Chapin et al. 2005). In particular, wildfires may affect the ongoing

shrubification (i.e. increased cover, abundance, and biomass of shrubs) of the tundra, which has the potential to counterbalance carbon stock losses from permafrost soils (Mekonnen et al. 2018; Gagnon et al. 2019).

Despite well-established linkages between climate change and shrubification (e.g. Myers-Smith et al. 2015; Martin et al. 2017), the influence of wildfire on shrub expansion across heterogeneous tundra terrain remains uncertain (Moritz et al. 2012; Young et al. 2017). Previous studies generally suggest that fire disturbance will strengthen shrubification by removing competing vegetation, exposing shrub seedbeds, and accelerating nutrient mineralization (Heim et al. 2019; Lantz et al. 2010; Mekonnen et al. 2019; Racine et al. 2004). However, it is unclear whether these results are representative of all tundra ecosystems, as substantial spatial heterogeneity in topography (Lara et al. 2015), microclimate (Harris et al. 2014) and permafrost condition (Pastick et al. 2015) may dynamically modulate fire-shrub interactions. For example, in a lowland riparian tundra, permafrost degraded four years after shrub removal, which caused the ground to subside and infill with surface water (i.e. thermokarst) that eventually drowned an abundance of adjacent intact shrubs (Li et al. 2017; Nauta et al. 2015). Since both fire disturbance and climate change can destabilize permafrost (Jones et al. 2015, Lara et al. 2019) and exert strong influences on shrub cover (Mekonnen et al. 2018; Gagnon et al. 2019; Li et al. 2017; Nauta et al. 2015), our knowledge of climate-fire-permafrost interactions that control shrub-cover dynamics is limited.

This study aims to unravel the spatially heterogeneous and temporally dynamic associations between fire disturbance and climate change on shrub cover in the Noatak National Preserve (NOAT, 67.5^{o} N, 162.6^{o} W, Fig. 1e) of northern Alaska. The NOAT was selected for this study as (1) it is among the most flammable tundra ecosystems on Earth (Higuera et al. 2011; Rocha et al. 2012), (2) has experienced marked climatic warming over recent decades (Sousanes & Hill 2017), and (3) is underlain by variable ground-ice content that generally increase from tundra uplands to lowlands (Shur & Jorgenson 2007, Olefeldt et al. 2016). This combination of environmental factors presents us with the unique opportunity to investigate how climate change, fire disturbance, and landscape attributes may modulate shrub-cover dynamics across high-latitude tundra ecosystems.

2. MATERIALS AND METHODS

2.1 Study sites

The NOAT spans an area of 2.9×10^4 km^2 in northwestern Alaska (Fig. 1e). According to the nearest meteorological station (1980-2020) at the Kotzebue Airport (30 km from NOAT), the region is relatively warm and arid with a mean growing-season (June, July and August) temperature of 10.6 ^{o}C and a total growing-season precipitation of 108.3 mm. The NOAT is among the warmest tundra ecosystems on earth (Harris et al. 2014), and it has experienced substantial warming (+2.1 ^{o}C) since 1950 (Sousanes & Hill 2017). This region has an active fire regime over the past 2,000 years with estimated mean fire return interval around 200 years (Higuera et al. 2011). The ground-ice content in the NOAT is highly variable, closely associated with topographical gradients and land cover types (Jorgenson et al. 2014). The shrubs we monitored in the NOAT are rapidly expanding "tall shrubs", from the genera of *Salix*, *Betula*, and *Alnus* (Swanson 2015). Although the extent of all three shrub taxa is rapidly changing in the NOAT, *Salix* dominates upland environments, whereas *Betula* is the most common species in lowland NOAT (Swanson 2015).

We investigated fire-shrub interactions within four historical tundra fires (OTZ-NNW38 Fire, OTZ-NE100 Fire, S-Noatak Fire, and IAN-NE25 Fire; AICC https://fire.ak.blm.gov/) in the NOAT (Fig. 1 a-d). The fires were selected based on their time of occurrence (>2 decades ago, for reliable change detection; AICC 1950-2020), fire severity levels (burned in high to low severity; MTBS 1984-2020, Chen et al. 2020), and landscape attributes (land cover and drainage conditions; Frost & Epstein 2014, Raynolds et al. 2017). The OTZ-NNW38 Fire (67.5^o N, 162.8^o W) occurred in 1977 (Fig. 1a), burning an area of 459.5 km^2 across poorly-drained (slope < 2^o; Frost & Epstein 2014) and ice-rich lowland tundra (Raynolds et al. 2017). It is the largest lowland fire on record with a size ~40 times an average Alaskan tundra fire (Chen et al. 2020). This single fire accounted for ~90% of poorly-drained lowlands burned since 1950 in the NOAT, or ~70% in the entire Arctic Alaska (AICC 1950-2020). Within the perimeter of the OTZ-NNW38 Fire, 43%, 50%, and 7% of the area was classified as low, moderate, and high fire severity, respectively (Fig. 1a, Chen et al. 2020). The OTZ-NE100 Fire (68.1^o N, 159.4^o W) occurred in 1986 (Fig. 1b), burning an area of 21.8 km^2 along gently sloping, well-drained upland tundra (Raynolds et al. 2017). Nearly one-half of the burned area in the OTZ-NE100 Fire was characterized by low severity (48%), followed by moderate (39%), and high (13%) severity (Fig. 1b, MTBS 1984-2020). The S-Noatak Fire (68.0^o N, 159.7^o W) burned an area of 3.3 km^2 across

well-drained upland tundra in 1976 (Fig. 1c). This fire was characterized by low (2.6 km^2) to moderate (0.7 km^2) fire severity. Similarly, the IAN-NE25 Fire (68.1° N, 159.5° W) was a relatively small upland tundra fire (1.0 km^2) burning primarily in low (0.4 km^2) to moderate (0.6 km^2) severity in 1982 (Fig. 1d).

We selected our study sites (250 × 250 m, n = 114) in both burned and the adjacent unburned tundra (Fig. 1 a-d) to separate the effects of fire disturbance from that of climate change on shrub-cover dynamics. All sites were placed with a minimum distance of 500 m apart from one another. The unburned sites were located in areas greater than 500 m and less than 2,000 m radius surrounding the fire perimeters (Fig. 1 a-d). To achieve an unbiased representation of tundra types (upland and lowland tundra) and fire severity levels (high, moderate, low, and unburned), we utilized a stratified random sampling algorithm to assign our study sites to each tundra type × fire severity group (Fig. 1 a-d).

2.2 Image acquisition and preprocessing

We acquired 117 historical (1951 to 1988) black and white aerial photos (resolution of 0.5 ~ 1.5 m, collected by NASA AMES Research Center and NASA Johnson Space or by the Keyhole satellite system KH-9) and 10 recent (2007 to 2016) panchromatic (resolution of 0.3 ~ 1.0 m) and the associated multispectral (resolution of 1.7 ~ 3.2 m) satellite images (collected by commercial satellites Quickbird-2, Worldview-2, Ikonos and Geoeye-1). All aerial photos and satellite images were obtained during the growing season, with a spatial resolution adequate for identifying individual shrub canopies (< 2 m, Frost et al. 2013). Image coverage for the OTZ-NNW38 Fire was available in year 1951 and 1976 (pre-fire), and 2007 (post-fire). The years with image coverage for the OTZ-NE100 Fire was 1977 (pre-fire), and 2007 and 2016 (post-fire). The S-Noatak Fire and the IAN-NE25 Fire were covered by images acquired in 1971 (pre-fire) and 2007 (post-fire). Image orthorectification and co-registration were conducted according to the protocol given by Necsoiu et al. (2013), which achieved an overall registration root mean square error between 0.001 to 0.8 m.

2.3 Time-series analysis of shrub cover dynamics

We quantified recent shrub cover distribution using a supervised support vector machine classifier (ArcGIS 10.5) on pansharpened (0.3~1.0 m) multispectral images (Table 1) following Lara et al. (2018, 2019). Briefly, we selected 15 – 25 training samples across each image to represent shrub and

non-shrub (e.g. water body, graminoid, wetland, and barren) land cover. The classification outputs were compared against the pansharpened images at reference sites generated by gridding the burned and unburned tundra at 250 × 250 m pixel. Overall, our classification achieved a *Producer's* accuracy of 85.1 ± 4.6% and 92.1 ± 2.5%, and the *User's* accuracy of 81.0 ± 5.1% and 94.3 ± 1.4% for shrub and non-shrub land cover, respectively (Table 1).

We assessed historical shrub cover captured in single-band aerial photos in two steps. First, we extracted shrub cover from grey-scale images by thresholding dark pixels corresponding to clusters of dark leaves and canopy shadows of shrub patches (e.g. Frost et al. 2013). Shrubs are readily identifiable on high-resolution imagery by using a combination of shape, size, texture, and distribution of pixels (Frost et al. 2013; Frost & Epstein 2014, Lara et al. 2018). Second, we compared the historical shrub extent to recent pansharpened multispectral images to manually remove potential confounding features such as small water bodies and terrain shadows that possess brightness characteristics resembling shrubs in grey-scale images.

2.4 Data analysis

Prior to analysis we normalized all shrub-cover estimates to square meter per hectare (m^2 ha^{-1}). The rate of shrub area change (m^2 ha^{-1} yr^{-1}) within any given time interval was computed as the differenced shrub area divided by the number of years between the time interval. To account for repeated measures, we applied mixed-design ANOVA to evaluate the differences in shrub-cover dynamics between time interval and between fire severity, in which time interval is the within-subjects factor and fire severity the between-subjects factor. The degrees of freedom were adjusted by the Greenhouse-Geisser adjustment method for the sphericity of the covariance matrix assumption. Differences were considered significant at $p < 0.05$.

We then selected 24 candidate explanatory variables for shrub-cover dynamics identified from the literature and the present study (Table 2). These variables can be grouped into five broad categories, (1) meteorological variables, such as temperature and precipitation; (2) ground and belowground variables, including active layer depth and soil temperature; (3) topographic variables, such as topographic position index and permafrost probability; (4) fire severity; and (5) landscape metrics, such as proximity to nearest river or stream (Table 2).

Our approach was to initially fit a multivariate linear regression model that included all candidate variables, and then remove unimportant variables in a stepwise fashion until a single reduced model was achieved that only retained significant factors ($p < 0.05$) for our response variable (rate of shrub area change, $m^2\ ha^{-1}\ yr^{-1}$). A single regression model was created if burned and unburned tundra had a similar directional change in shrub cover over time. If the trajectories of shrub-cover change diverged between burned and unburned tundra, two separate regression models were generated to describe the distinct patterns of shrub-cover change in the presence and absence of fire. *Pearson's* correlation coefficients (r) were computed between the response variable and the set of predictors retained in the final models. The adjusted coefficient of determination (R^2_{adj}) was used to indicate the explanatory power of the models.

The accuracy of the predictive models was independently validated with data from 22 sites (250 × 250 m) that were randomly placed across the OTZ-NNW38 Fire and four additional tundra fires in the NOAT: two fires in the uplands and two in the lowlands (Fig. 1e and Table 3). Similar to our fire selection criteria mentioned previously, the validation sites were selected based on image availability, time of fire occurrence, fire severity, and tundra types (Table 3). The unburned sites were situated in areas greater than 500 m but less than 2,000 m radius outside the fires. For each validation site, we acquired two high-resolution (~1.0 m) aerial photos or satellite images (Table 3) to analyze the rate of shrub-cover change ($m^2\ ha^{-1}\ yr^{-1}$) following the same procedure described earlier. All geoprocessing was performed in ArcGIS 10.5, and all data analyses was completed in R (v 3.6.1).

3. RESULTS

Shrub cover was minimal (128.4 ± 13.2 $m^2\ ha^{-1}$, $n = 66$) across upland tundra, approximately one decade prior to fire occurrence (Figs. 2-3). In unburned areas, upland shrub cover increased at a slow rate of 3.3 ± 1.3 $m^2\ ha^{-1}\ yr^{-1}$ ($n = 15$) during the first two postfire decades (Fig. 2), and at an elevated rate of 6.3 ± 1.4 $m^2\ ha^{-1}\ yr^{-1}$ ($n = 12$) during the third decade (Fig. 2). In burned upland tundra, shrub expansion greatly accelerated after fire (Figs. 2-3), and the rates differed significantly ($F = 23.67$, $p < 0.001$) between high, and moderate-low severity burns. In high-severity burns, the rate of shrub expansion reached 56.4 ± 6.0 $m^2\ ha^{-1}\ yr^{-1}$ ($n = 12$) during the first two postfire decades, compared to 37.6 ± 4.2 $m^2\ ha^{-1}\ yr^{-1}$ ($n = 14$) at moderate-severity burns and 21.7 ± 2.9 $m^2\ ha^{-1}\ yr^{-1}$ ($n = 13$) at low-severity burns (Fig. 2). The rate of shrub expansion during the third postfire decade decreased by

7.6% from that during the first two decades, but remained 7.3, 4.7, and 3.0 times the rate of unburned uplands for high, moderate, and low-severity burns, respectively (Fig. 2). When averaged across burned uplands (n = 45), the shrub cover increased by 1077.2 ± 83.6 m^2 ha^{-1} over three postfire decade, an amount nearly seven-fold the increase in unburned tundra (155.1 ± 55.4 m^2 ha^{-1}, n = 21) (Figs. 2-3).

The patterns of shrub-cover change in lowland tundra differed from those in the uplands (Figs. 2-4). Lowland shrubs were already expansive (930.4 ± 78.6 m^2 ha^{-1}, n = 48, Figs. 2 and 4) two decades prior to fire occurrence. The shrub cover in unburned lowlands expanded rapidly, at a rate of 18.0 ± 3.6 m^2 ha^{-1} yr^{-1} (n = 12) during the three postfire decades (Fig. 2). By 2007 (Years since fire = 30, Fig. 2), lowland shrub cover in unburned tundra was 1857.4 ± 324.1 m^2 ha^{-1} (n = 12), approximately an order of magnitude higher than contemporary unburned uplands (179.7 ± 60.5 m^2 ha^{-1}, n = 12, Fig. 2). In contrast, shrub cover in burned lowlands drastically declined after fire (Figs. 2 and 4), but no difference was found between fire severity levels (F = 0.56, p = 0.79). Shrub cover in burned lowlands decreased at a rapid rate of 23.1 ± 2.3 m^2 ha^{-1} yr^{-1} (n = 36) during the three postfire decades, corresponding to 52.9% shrub-cover loss from 1977 (1309.2 ± 122.8 m^2 ha^{-1}, n = 36, Years since fire = 0) to 2007 (616.4 ± 74.1 m^2 ha^{-1}, n = 36) (Fig. 2). As a result, the shrub cover in burned lowlands by 2007 was only 33.2% of that in unburned lowlands, or 64.4% of that in contemporary burned uplands (Figs. 2-4).

Our multivariate regression models captured the majority of the variability in shrub-cover change across upland and lowland tundra ($R^2_{adj.} \geq 0.67$, $p < 0.001$, Fig 5). In both burned and unburned upland tundra, we identified a similar positive directional change in shrub cover over time (Figs 2-3). The patterns of shrub-cover change in unburned and burned uplands were well-explained by a single regression model ($R^2_{adj.}$ = 0.76, $p < 0.001$; Fig. 5) with three most influential variables: fire severity (r = 0.83, $p < 0.001$), total summer precipitation (TSP, r = 0.67, $p < 0.001$), and initial shrub area (Area, r = 0.34, p = 0.005), which respectively accounted for 43.6%, 30.8%, and 15.5% of the observed variance (Fig. 5). The modeled shrub-cover change in upland tundra agreed well with our observations from two validation fires (Fig. 5, Table 3), showing rapid increase of shrub cover in severely burned area and relatively small changes in unburned tundra. This result lent confidence to our upland model in capturing shrub-cover change across a gradient of fire severity levels.

Shrub-cover change in the lowlands had an opposite temporal trajectory between burned (contraction) and unburned (expansion) tundra (Figs. 2 and 4). In burned lowlands, our model (Lowland-burned, $R^2_{adj.}$ = 0.70, p < 0.001, Fig. 5) indicated that the rate of shrub-cover change was dictated by mean summer air temperature (MSAT, r = -0.82, p < 0.001), permafrost probability (Permafrost, r = -0.60, p < 0.001), and length of growing season (LOGS, r = -0.63, p < 0.001; Fig. 5). MSAT, Permafrost, and LOGS contributed 28.1%, 23.4% and 16.6% to the overall variance of shrub cover in burned lowland, respectively (Fig. 5). On the contrary, shrub cover in unburned lowlands (Lowland-unburned, Fig. 5) increased with increasing MSAT (r = 0.78, p < 0.001) and Area (r = 0.53, p < 0.001), and with decreasing TSP (r = -0.56, p < 0.001), which accounted for 28.8%, 15.6% and 10.0% of the observed variance, respectively ($R^2_{adj.}$ = 0.67, p < 0.001, Fig. 5). The performance of the lowland models was confirmed by our validation sites (Table 3) from the OTZ-NNW38 Fire and two other lowland fires (Fig. 5). The overall agreement in shrub-cover change between our simulations and the range of observations from burned and unburned tundra provided credence that our models can reproduce the variability of shrub-over change in the presence or absence of fire in the lowlands.

4. DISCUSSION

The spatiotemporal patterns of shrub-cover dynamics captured by this study unveiled divergent pathways of shrub-cover responses to fire disturbance and climate change. In unburned tundra, our analysis revealed widespread increase in shrub cover over the past few decades (Figs. 2-4), and the rate of change was strongly mediated by topographical position and climatic factors (Figs. 5-6). Shrub expansion in unburned uplands was consistenly outpaced by unburned lowlands despite similar warming trends across NOAT (Sousanes & Hill 2017). The shrub cover in fire-free lowlands was most responsive to summer warming, which alone accounted for 28.8% of overall variance (Fig. 5). In contrast, shrub cover in unburned uplands was intimately linked to precipitation that largely outweighed summer temperature (3.2%) and was responsible for over 30% of shrub-cover change (Fig. 5). These contrasting results between lowland and upland tundra likely reflect their distinct soil moisture regimes (Raynolds et al. 2017). Previous studies suggested that the lack of soil moisture impedes shrub colonization in dry hillslope tundra (Frost & Epstein 2014; Piao et al. 2006), and elevated drought stress is usually associated with lowered temperature sensitivity of tundra shrubs (Piao et al. 2014; Elmendorf et al. 2012; Tape et al. 2012; Tremblay et al. 2012). Given the observed

patterns and future climatic projections (Harris et al. 2014), our results imply that shrubs may continue to flourish in mesic lowland tundra as long as favorable soil moisture persists, whereas amplified drought risks assocated with warming climate in upland tundra (Box et al. 2019; Andresen et al. 2020) may pose growing obstacles for shrub encroachment.

Fire disturbance strongly interacted with climate change to shape the spatial and temporal patterns of shrub distribution, but the magnitude and direction of shrub-cover change depend on landscape position. In tundra uplands, we observed that shrub expansion greatly accelerated after fire disturbance (Figs. 2-3). This finding is consistent with many field observations that wildfire facilitates tundra shrubification (e.g. Heim et al. 2019; Jeffers et al. 2012; Lantz et al. 2010; Racine et al. 2004), and our remote-sensing monitoring extends postfire observation to 30 years that uncovered enduring legacy of wildfire on tundra vegetation. Moreover, we captured strong positive correspondence between fire severity and shrub expansion in the uplands (Figs. 2 and 5), adding an extra layer of understanding to fire-shrub interactions in tundra ecosystem. These results may be particularly important as projected climate change will not only increase fire frequency but also fire severity (Mann et al., 2012), which may hasten shrubification across tundra uplands.

The enhanced expansion of shrubs in disturbed uplands likely benefited from the relaxation of resource limitation following permafrost degradation (Fig. 3). Thawing permafrost associated with fire disturbance might have enhanced soil moisture (as indicated by extensive drainage networks forming shortly after fire) and potentially catelyzed nitrogen mineralization to boost shrub colonization across tundra uplands (Heim et al. 2019; Lantz et al. 2010; Racine et al. 2004; Mekonnen et al. 2019). The expansion of shrubs may in turn expedite nitrogen turnover via greater nitrogen uptake (DeMarco et al. 2014), higher quantity and quality of plant litter (Vankoughnett and Grogan 2016; McLaren et al. 2017) and by snow interception that allows year-round microbial decomposition (DeMarco et al. 2011). These processes can strongly modify soil biogeochemistry and biophysics (Weintraub and Schimel 2005; Vowles and Björk 2019), which might have fueled persistent shrub proliferation manifested in burned uplands. These results, in conjunction with prior studies linking shrubification with heightened landscape flamability (Higuera et al. 2008, 2011; Jeffers et al. 2012; Rocha et al. 2012), depict a postive feedback loop for upland tundra ecosystem between rapid shrub expansion and severe wildfires in the decades to come (Fig. 6).

Shrubs in the ice-rich tundra lowlands largely disappeared after fire disturbance, starkly contrasting with expanding shrub patches in unburned lowlands and burned uplands (Figs. 2-4). This novel finding strongly suggests that tundra fire, even at low severity, has the potential to temporarily or even permanently reverse the trajectory of shrub expansion at local to regional scales. The steady decline of lowland shrubs in the years to decades after fire was associated with the progressive collapse of ice-rich permafrost (i.e. thermokarst), followed by rapid water impounding under poorly drained conditions – a process also seen in some boreal lowlands (Jorgenson & Osterkamp 2005, Brown et al. 2015). Such changes in microrelief and soil hydrology can strongly inhibit nutrient cycling (Myers-Smith et al. 2008) and destroy moisture optima for shrub growth and recruitment (Nauta et al. 2015).

More interestingly, we found that warming climate contributed to shrub-cover losses in burned lowlands, as opposed to facilitating shrub expansion in unburned lowlands (Figs. 5-6). This finding supports the hypothesis that shrub cover and permafrost are interdependent in low-lying environments (e.g. Nauta et al. 2015; Li et al. 2017). Studies in ice-rich Arctic terrains revealed that summer shading of shrubs enhanced insulation for permafrost, allowing it to persist in a warmer world (Liljedahl et al. 2016; Osterkamp et al. 2000). In the unburned lowlands where shrub cover remained intact, no thermokarst was detected despite substantial regional warming since 1950 (~2 ^{o}C, Sousanes & Hill 2017). This result support dense shrubs as an effective insulating blanket buffering permafrost from changing climate. However, soil insulation may be weakened after shrub cover is removed (Nauta et al. 2015; Kokelj and Jorgenson 2013), which potentially promoted permafrost degradation and furthered shrub-cover losses by perpetuating a positive feedback to permafrost thaw (Fig. 6). This process likely explained the ~ 50% decline of shrub cover throughout three postfire decades in burned tundra lowlands (Figs. 2 and 4). Given the efficacy of wildfire in consuming shrubs and exacerbating soil warming (Rocha et al. 2012; Hu et al. 2015), it is likely that fire-regime change will represent a burgeoning source of uncertainty in biogeochemistry models as it disrupts future shrub and permafrost distribution across lowland tundra environments.

5. CONCLUSION

Although the NOAT selected by our study is among the most flammable tundra ecosystems on earth, our current understanding of fire-shrub interaction remains limited by the inherent paucity of tundra

fires in general (Hu et al. 2015; Chipman et al. 2015). This is especially true for ice-rich, poorly-drained lowlands where fire disturbance has been historically rare due to saturated soils interspersed with numerous lakes, ponds, bogs and fens that strongly inhibit fire ignition and spread (McCarty et al. 2020; Hu et al. 2015). As a result, our findings based upon five upland fires and three lowland fires should be interpreted with caution considering limited spatial extent of historical tundra fires (AICC 1950-2020) coupled with substantial spatial heterogeneity of tundra landscape (e.g. Hamilton 2010; Pastick et al. 2015).

Although uncertainties remain large, our 40+ years monitoring of shrub-cover change from contrasting landscape settings provides novel insights into the vegetation-wildfire interactions in the rapidly warming tundra ecosystem, highlighting 1) that the responses of tundra vegetation to climate change may have multiple trajectories depending on landscape attributes, and 2) that activating wildfire may increasingly influence the direction and magnitude of future shrub-cover in high latitudes. With projected increase in the range and magnitude of tundra fires in this century (Young et al. 2017; Moritz et al. 2012), we expect that additonal confidence in the dynamics of tundra vegetation will be gained by future studies that encompass fires from complex landscape components.

ACKNOWLEDGEMENTS

Funding for this research was provided by the NSF (1023477, 1636476 to F.S.H, and 1928048 to M.J.L). We are grateful for the geospatial support provided for this work by the Polar Geospatial Center under NSF PLR awards 1043681 & 1559691. Any use of trade, firm, or product names is for descriptive purposes only and does not imply endorsement by the U.S. Government.

CONFLICT OF INTEREST

The authors declare no conflict of interest.

AUTHOR CONTRIBUTION

Y.C. led all aspects of the study; Y.C. and M.J. L. designed the study, carried out laboratory work and performed statistical analyses; all authors interpreted data and drafted the manuscript.

DATA AVAILABILITY STATEMENT

All data reported here are available at NSF Arctic Data Center (https://arcticdata.io/).

ORCID

Yaping Chen https://orcid.org/0000-0003-1372-8861

REFERENCES

Ackerman, D., Griffin, D., Hobbie, S. E., & Finlay, J. C. (2017). Arctic shrub growth trajectories differ across soil moisture levels. Global Change Biology 23(10): 4294–4302. https://doi.org/10.1111.

AICC – Alaska Interagency Coordination Center, 1943-2020. https://fire.ak.blm.gov/. (accessed June 20, 2020).

Andresen, C. G., Lawrence, D. M., Wilson, C. J., McGuire, A. D., et al. (2020). Soil moisture and hydrology projections of the permafrost region-a model intercomparison. Cryosphere 14(2): 445–59. https://doi.org/10.5194/tc-14-445-2020.

Berner, L. T., Jantz, P., Tape, K. D., & Goetz, S. J. (2018). Tundra plant above-ground biomass and shrub dominance mapped across the North Slope of Alaska. Environmental Research Letters 13(3). https://doi.org/10.1088/1748-9326/aaaa9a.

Blok, D., Heijmans, M. M. P. D., Schaepman-Strub, G., Kononov, A. V., Maximov, T. C., & Berendse, F. (2010). Shrub expansion may reduce summer permafrost thaw in Siberian tundra. Global Change Biology 16(4): 1296–1305. https://doi.org/10.1111/j.1365-2486.2009.02110.x.

Box, J. E., Colgan, W. T., Christensen, T. R., Schmidt, N. M., Lund, M., et al. (2019). Key indicators of Arctic climate change: 1971-2017. Environmental Research Letters 14(4). https://iopscience.iop.org/article/10.1088/1748-9326/aafc1b.

Brown, D., Jorgenson., M. T., Douglas, T., & Ruess, R. (2015). Interactions of fire and climate exacerbate permafrost degradation in Alaskan lowland forests. Journal of Geophysical Research, Biogeosciences 120: 1619– 1637. https://doi.org/10.1002/2015JG003033.

Chen, Y., Lara, M. J., & Hu, F. S. (2020). A robust visible near-infrared index for fire severity mapping in Arctic tundra ecosystems. ISPRS Journal of Photogrammetry and Remote Sensing 159: 101–13. https://doi.org/10.1016/j.isprsjprs.2019.11.012.

Chipman M. L., Hudspith V., Higuera P. E., Duffy P. A., Kelly R., Oswald W. W. & Hu F. S. (2015). Spatiotemporal patterns of tundra fires: late-Quaternary charcoal records from Alaska. Biogeosciences 12: 4017–4027, https://doi.org/10.5194/bg-12-4017-2015.

Danielson, J. J., & Gesch, D. B. (2011). Global multi-resolution terrain elevation data 2010 (GMTED2010): U.S. Geological Survey Open-File Report 2011–1073, 26 p. https://pubs.usgs.gov/of/2011/1073/pdf/of2011-1073.pdf.

DeMarco, J., Mack, M. C., & Bret-Harte, M. S. (2011). The effects of snow, soil microenvironment, and soil organic matter quality on N availability in three Alaskan Arctic plant communities. Ecosystems 14: 804–817. https://doi.org/10.1007/s10021-011-9447-5.

DeMarco, J., Mack, M. C., & Bret-Harte, M. S. (2014). Effects of arctic shrub expansion on biophysical vs. biogeochemical drivers of litter decomposition. Ecology 95: 1861–1875. https://doi.org/10.1890/13-2221.1.

Eidenshink, J., Schwind, B., Brewer, K., et al. (2007). A project for monitoring trends in burn severity. Fire Ecology 3: 3-21. https://doi.org/10.4996/fireecology.0301003.

Elmendorf, S. C., Henry, G. H. R., Hollister, R. D., et al. (2012). Plot-scale evidence of tundra vegetation change and links to recent summer warming. Nature Climate Change 2(6): 453–57. https://doi.org/10.1038/nclimate1465.

Epstein, H. E., Raynolds, M. K., Walker, D. A., Bhatt, U. S., et al. (2012). Dynamics of aboveground phytomass of the circumpolar Arctic tundra during the past three decades. Environmental Research Letters 7(1). https://iopscience.iop.org/article/10.1088/1748-9326/7/1/015506.

Frost, G. V., & Epstein, H. E. (2014). Tall shrub and tree expansion in Siberian tundra ecotones since the 1960s. Global Change Biology 20(4): 1264–77. https://doi.org/10.1111/gcb.12406.

Frost, G. V., Epstein, H. E., Walker, D. A., Matyshak, G., & Ermokhina, K. (2013). Patterned ground facilitates shrub expansion in low Arctic tundra. Environmental Research Letters 8(1). https://iopscience.iop.org/article/10.1088/1748-9326/8/1/015035.

Gagnon, M., Domine, F., & Boudreau, S. (2019). The carbon sink due to shrub growth on Arctic tundra: a case study in a carbon-poor soil in eastern Canada. Environmental Research Communications 1(10): 109501. https://iopscience.iop.org/article/10.1088/2515-7620/ab3cdd.

Hamilton, T. D. (2010). Surficial geologic map of the Noatak national preserve, Alaska. U.S. Geological Survey Scientific Investigations Map 3036. https://pubs.usgs.gov/sim/3036/.

Harris, I., Jones, P. D., Osborn, T. J., & Lister, D. H. (2014). Updated high-resolution grids of monthly climatic observations - the CRU TS3.10 Dataset. International Journal of Climatology 34(3): 623–42. https://doi.org/10.1002/joc.3711.

Heim, R. J., Bucharova, A., Rieker, D., Yurtaev, A., Kamp, J., & Hölzel, N. (2019). Long-term effects of fire on Arctic tundra vegetation in western Siberia. bioRxiv 1–33. https://doi.org/10.1101/756163.

Higuera, P. E., Brubaker, L. B., Anderson, P. M., et al. (2008). Frequent fires in ancient shrub tundra: implications of paleorecords for arctic environmental change. PLoS ONE 3(3): 1–7. https://doi.org/10.1371/journal.pone.0001744.

Higuera, P. E., Chipman, M. L., Barnes, J. L., Urban, M. A., & Hu, F. S. (2011). Variability of tundra fire regimes in Arctic Alaska: millennial-scale patterns and ecological implications. Ecological Applications 21(8): 3211–26. https://doi.org/10.1890/11-0387.1.

Homer, C., Dewitz, J., Yang, L., Jin, S., Danielson, P., Xian, G., Coulston, J., et al. (2015). Completion of the 2011 national land cover database for the conterminous United States – representing a decade of land cover change information. Photogrammetric Engineering and Remote Sensing 81: 345–353. https://doi.org/10.14358/PERS.81.5.345.

Hu, F. S., Higuera, P. E., Duffy, P., et al. (2015). Arctic tundra fires: natural variability and responses to climate change. Frontiers in Ecology and the Environment 13(7): 369–77. https://doi.org/10.1890/150063.

Huebner, D. C., & Bret-Harte, M. S. (2019). Microsite conditions in retrogressive thaw slumps may facilitate increased seedling recruitment in the Alaskan Low Arctic. Ecology and Evolution 9(4): 1880–1897. https://doi.org/10.1002/ece3.4882.

Jeffers, E. S., Bonsall, M. B., Watson, J. E., & Willis, K. J. (2012). Climate change impacts on ecosystem functioning: evidence from an *Empetrum* heathland. New Phytologist 193(1): 150–64. https://doi.org/10.1111/j.1469-8137.2011.03907.x.

Jones, B.M., Grosse, G., Arp, C.D., et al., 2015. Recent Arctic tundra fire initiates widespread thermokarst development. Sci. Rep. 5, 15865. https://www.nature.com/articles/srep15865.

Jorgenson, M. T., et al. 2014. U.S. Fish and Wildlife Service, Arctic Landscape Conservation Cooperative Permafrost Database Development, Characterization, and Mapping for Northern Alaska. Anchorage, AK. http://arcticlcc.org/projects/ALCC2012-10.

Jorgenson, M. T., & Osterkamp, T. E. (2005). Response of boreal ecosystems to varying modes of permafrost degradation. Canadian Journal of Forest Research 35(9): 2100–2111. https://doi.org/10.1139/x05-153.

Kokelj, S. V., & Jorgenson, M. T. (2013). Advances in thermokarst research. Permafrost and Periglacial Processes 24(2): 108–19. https://doi.org/10.1002/ppp.1779.

Lantz, T. C., Gergel, S. E., & Henry, G. H. R. (2010). Response of green alder (*Alnus Viridis* Subsp. *Fruticosa*) patch dynamics and plant community composition to fire and regional temperature in north-western Canada. Journal of Biogeography 37(8): 1597–1610. https://doi.org/10.1111/j.1365-2699.2010.02317.x.

Lara, M. J., Mcguire, A. D., Euskirchen, E. S., Tweedie, C. E., et al. (2015). Polygonal tundra geomorphological change in response to warming alters future CO_2 and CH_4 flux on the Barrow Peninsula. Global Change Biology 21(4): 1634–51. https://doi.org/10.1111/gcb.12757.

Lara, M. J., Nitze, I., Grosse, G., & McGuire, A. D. (2018). Data descriptor: tundra landform and vegetation productivity trend maps for the Arctic coastal plain of northern Alaska. Scientific Data 5: 1–10. https://doi.org/10.1038/sdata.2018.58.

Lawrence, D. M., & Swenson, S. C. (2011). Permafrost response to increasing Arctic shrub abundance depends on the relative influence of shrubs on local soil cooling versus large-scale climate warming. Environmental Research Letters 6. https://doi.org/10.1088/1748-9326/6/4/045504.

Li, B., Heijmans, M. M. P. D., Blok, D., Wang, P., et al. (2017). Thaw pond development and initial vegetation succession in experimental plots at a Siberian lowland tundra site. Plant and Soil 420(1–2): 147–62. https://doi.org/10.1007/s11104-017-3369-8.

Liljedahl, A. K., Boike, J., Daanen, R. P., Fedorov, A. N., et al. (2016). Pan-Arctic ice-wedge degradation in warming permafrost and its influence on tundra hydrology. Nature Geoscience 9(4): 312–18. https://doi.org/10.1038/ngeo2674.

Lindsay, C., Zhu, J., Miller, A. E., Kirchner, P., & Wilson, T. L. (2015). Deriving snow cover metrics for Alaska from MODIS. Remote Sensing 7(10): 12961–85. https://doi.org/10.3390/rs71012961.

Luo, D. L., Jin H., Marchenko, S., & Romanovsky, V. (2014). Distribution and changes of active layer thickness (ALT) and soil temperature (TTOP) in the source area of the Yellow River using the GIPL model. Science China Earth Sciences 57(8): 1834–45. https://doi.org/10.1007/s11430-014-4852-1.

Mack, M. C., Bret-Harte, M. S., Hollingsworth, T. N., et al. (2011). Carbon loss from an unprecedented Arctic tundra wildfire. Nature 475(7357): 489–92. https://doi.org/10.1038/nature10283.

Mann, D., Rupp, T., Olson, M., & Duffy, P. (2012). Is Alaska's boreal forest now crossing a major ecological threshold? Arctic, Antarctic, and Alpine Research 44(3): 319–31. https://doi.org/10.1657/1938-4246-44.3.319.

Martin, A. C., Jeffers, E. S., Petrokofsky, G., et al. (2017). Shrub growth and expansion in the Arctic tundra: an assessment of controlling factors using an evidence-based approach. Environmental Research Letters 12(8): 2000–2010. https://iopscience.iop.org/article/10.1088/1748-9326/aa7989.

McCarty, J. L., Smith, T. E. L. & Turetsky, M. R. (2020). Arctic fires re-emerging. Nature Geoscience 13: 658–660. https://doi.org/10.1038/s41561-020-00645-5.

McKay, L., Bondelid, T., Dewald, T., Johnston, J., Moore, R., & Rea, A. (2019). NHDPlus Version 2: User guide (Data Model Version 2.1). 182. https://www.ingentaconnect.com/content/asprs/pers/.

McLaren, J. R., Buckeridge, K. M., Van De Weg, M. J., Shaver, G. R., Schimel, J. P., & Gough, L. (2017). Shrub encroachment in Arctic tundra: *Betula nana* effects on above- and belowground litter decomposition. Ecology 98: 1361–1376. https://doi.org/10.1002/ecy.1790.

Mekonnen, Z. A., Riley, W. J., & Grant, R. F. (2018). 21st century tundra shrubification could enhance net carbon uptake of north America Arctic tundra under an RCP8.5 climate trajectory. Environmental Research Letters 13(5). https://iopscience.iop.org/article/10.1088/1748-9326/aabf28.

Mekonnen, Z. A., Riley, W. J., Randerson, J. T., et al. (2019). Expansion of high-latitude deciduous forests driven by interactions between climate warming and fire. Nature Plants 5(9): 952–58. https://doi.org/10.1038/s41477-019-0495-8.

Michaelides, R. J., Schaefer, K., Zebker, H. A., Parsekian, A., et al. (2019). Inference of the impact of wildfire on permafrost and active layer thickness in a discontinuous permafrost region using the remotely sensed active layer thickness (ReSALT) algorithm. Environmental Research Letters 14(3): 35007. https://iopscience.iop.org/article/10.1088/1748-9326/aaf932.

Moritz, M. A., Parisien, M., Batllori, E., Krawchuk, M. A., van Dorn, J., Ganz, D. J., & Hayhoe, K. (2012). Climate change and disruptions to global fire activity. Ecosphere 3(6): art49. https://esajournals.onlinelibrary.wiley.com/doi/pdf/10.1890/ES11-00345.1.

MTBS – Monitoring Trends in Burn Severity, 1984-2020. https://www.mtbs.gov/. (accessed June 20, 2020).

Myers-Smith, I. H., Elmendorf, S. C., Beck, P. S. A., et al. (2015). Climate sensitivity of shrub growth across the tundra biome. Nature Climate Change 5(9): 887–91. https://doi.org/10.1038/nclimate2697.

Myers-Smith, I. H., Harden, J. W., Wilmking, M., Fuller, C. C., McGuire, A. D., and Chapin III, F. S. (2008). Wetland succession in a permafrost collapse: interactions between fire and thermokarst. Biogeosciences 5: 1273–1286. https://doi.org/10.5194/bg-5-1273-2008.

Myers-Smith, I. H., & Hik, D. S. (2018). Climate warming as a driver of tundra shrubline advance. Journal of Ecology 106(2): 547–560. https://doi.org/10.1111/1365-2745.12817.

Nauta, A. L., Heijmans, M. M. P. D., Blok, D., et al. 2015. Permafrost collapse after shrub removal shifts tundra ecosystem to a methane source. Nature Climate Change 5(1): 67–70. https://doi.org/10.1038/nclimate2446.

Necsoiu, M., Dinwiddie, C. L., Walter, G. R., et al. (2013). Multi-temporal image analysis of historical aerial photographs and recent satellite imagery reveals evolution of water body surface area and polygonal terrain morphology in Kobuk valley national park, Alaska. Environmental Research Letters 8(2). https://iopscience.iop.org/article/10.1088/1748-9326/8/2/025007.

Olefeldt, D., Goswami, S., Grosse, G. et al. (2016). Circumpolar distribution and carbon storage of thermokarst landscapes. Nature Communications 7: 13043. https://doi.org/10.1038/ncomms13043.

Osterkamp, T. E., Viereck, L., Shur, Y., Jorgenson, M. T., Racine, C., et al. (2000). Observations of thermokarst and its impact on boreal forests in Alaska, USA. Arctic, Antarctic, and Alpine Research 32(3): 303–15. https://doi.org/10.1080/15230430.2000.12003368.

Pastick, N. J., Jorgenson, M. T., Wylie, B. K., et al. (2015). Distribution of near-surface permafrost in Alaska: estimates of present and future conditions. Remote Sensing of Environment 168: 301–15. https://doi.org/10.1016/j.rse.2015.07.019.

Piao, S., Friedlingstein, P., Ciais, P., Zhou, L., & Chen, A. (2006). Effect of climate and CO_2 changes on the greening of the northern hemisphere over the past two decades. Geophysical Research Letters 33(23): 2–7. https://doi.org/10.1029/2006GL028205.

Piao, S., Nan, H., Huntingford, C., Ciais, P., et al. (2014). Evidence for a weakening relationship between interannual temperature variability and northern vegetation activity. Nature Communications 5: 1–7. https://doi.org/10.1038/ncomms6018.

Racine, C., Jandt, R., Meyers, C., & Dennis, J. (2004). Tundra fire and vegetation change along a hillslope on the Seward Peninsula, Alaska, USA. Arctic, Antarctic, and Alpine Research 36(1): 1–10. https://doi.org/10.1657/1523-0430(2004)036[0001:TFAVCA]2.0.CO;2.

Raynolds, M. K., Breen, A. L., & Walker, D. A. (2017). Land cover and ecosystem map collection for northern Alaska. ORNL DAAC, Oak Ridge, Tennessee, USA. https://doi.org/10.3334/ORNLDAAC/1359.

Rocha, A. V., Loranty, M. M., Higuera, P. E., et al. (2012). The footprint of Alaskan tundra fires during the past half-century: implications for surface properties and radiative forcing. Environmental Research Letters 7(4). https://iopscience.iop.org/article/10.1088/1748-9326/7/4/044039.

Schuur, E. A. G., Crummer, K. G., Vogel, J. G., et al. (2007). Plant species composition and productivity following permafrost thaw and thermokarst in Alaskan tundra. Ecosystems 10: 280–292. https://doi.org/10.1007/s10021-007-9024-0.

Serreze, M. C., & Barry, R. G. (2011). Processes and impacts of Arctic amplification: a research synthesis. Global and Planetary Change 77(1–2): 85–96. https://doi.org/10.1016/j.gloplacha.2011.03.004.

Shur, Y. L., & Jorgenson, M. T. (2007). Patterns of permafrost formation and degradation in relation to climate and ecosystems. Permafrost and Periglacial Processes 18(1): 7–19. https://doi.org/10.1002/ppp.582.

Sousanes, P. J., & Hill, K. (2017). Climate summary for the arctic parks. arctic inventory and monitoring network. Natural Resource Report NPS/ARCN/NRR–2017/1574. https://irma.nps.gov/Datastore/DownloadFile/593332.

Stehman, S. V. (1997). Selecting and interpreting measures of thematic classification accuracy. Remote Sensing of Environment 62(1): 77–89. https://doi.org/10.1016/S0034-4257(97)00083-7.

Sturm, M., Schimel, J., Michaelson, G., Welker, J. M., Oberbauer, S. F., Liston, G. E., et al. (2005). Winter biological processes could help convert Arctic tundra to shrubland. BioScience 55(1): 17. https://doi.org/10.1641/0006-3568(2005)055[0017:wbpchc]2.0.co;2.

Tape, K. D., Hallinger, M., Welker, J. M., & Ruess, R. W. (2012). Landscape heterogeneity of shrub expansion in Arctic Alaska. Ecosystems 15(5): 711–24. https://doi.org/10.1007/s10021-012-9540-4.

Tape, K. D., Sturm, M., & Racine, C. (2006). The evidence for shrub expansion in northern Alaska and the Pan-Arctic. Global Change Biology 12(4): 686–702. https://doi.org/10.1111/j.1365-2486.2006.01128.x.

Tremblay, B., Lévesque, E., & Boudreau, S. (2012). Recent expansion of erect shrubs in the low Arctic: evidence from eastern Nunavik. Environmental Research Letters 7(3). https://iopscience.iop.org/article/10.1088/1748-9326/7/3/035501.

Vankoughnett, M. R., & Grogan, P. (2016). Plant production and nitrogen accumulation above- and belowground in low and tall birch tundra communities: The influence of snow and litter. Plant and Soil 408: 195–210. https://doi.org/10.1007/s11104-016-2921-2.

Vowles, T., & Björk, R. G. (2019). Implications of evergreen shrub expansion in the Arctic. Journal of Ecology 107: 650– 655. https://doi.org/10.1111/1365-2745.13081.

Walker, M. D., Wahren, C. H., Hollister, R. D., Henry, G. H. R., et al. (2006). Plant community responses to experimental warming across the tundra biome. Proceedings of the National Academy of Sciences of the United States of America 103(5): 1342–1346. https://doi.org/10.1073/pnas.0503198103.

Weintraub, M. N., & Schimel, J. P. (2005). Nitrogen cycling and the spread of shrubs control changes in the carbon balance of Arctic tundra ecosystems. BioScience 55(5): 408–415. https://doi.org/10.1641/0006-3568(2005)055[0408:NCATSO]2.0.CO;2.

Young, A. M., Higuera, P. E., Duffy, P. A., & Hu, F. S. (2017). Climatic thresholds shape northern high-latitude fire regimes and imply vulnerability to future climate change. Ecography 40(5): 606–17. https://doi.org/10.1111/ecog.02205.

Zamin, T. J., & Grogan, P. (2012). Birch shrub growth in the low Arctic: The relative importance of experimental warming, enhanced nutrient availability, snow depth and caribou exclusion. Environmental Research Letters 7(3). https://doi.org/10.1088/1748-9326/7/3/034027.

TABLE 1. Image acquisition and accuracy assessment of supervised classification on multispectral satellite images. The *User's* accuracy and *Producer's* accuracy refers to Stehman (1997).

Tundra types	Image Acquisition			Classification Assessment		
	Time	**Resolution**	**Satellite**	**Accuracy index**	**Shrub**	**Non-shrub**
Upland	August 08, 2007	1.0 m	IKONOS	*User's* accuracy	78.0%	94.6%
	June 16, 2016	0.5 m	WorldView2	*User's* accuracy	88.1%	93.8%
	August 08, 2007	1.0 m	IKONOS	*Producer's* accuracy	79.6%	94.5%
	June 16, 2016	0.5 m	WorldView2	*Producer's* accuracy	88.8%	93.4%
Lowland	July 03, 2007	1.0 m	IKONOS	*User's* accuracy	76.7%	94.5%
	July 03, 2007	1.0 m	IKONOS	*Producer's* accuracy	88.0%	88.6%

TABLE 2. Selection of explanatory variables for modeling rate of shrub-cover change. Variables in bold are those retained in the final models.

Variable	Description	Data source	Reference
MAAT	Mean annual air temperature (°C)	CRU 4.0 (Harris et al. 2014)	
MSAT	Mean summer air temperature (°C)	CRU 4.0 (Harris et al. 2014)	Sturm et al. 2005; Walker et al. 2006; Elmendorf et al. 2012; Tremblay et al. 2012; Zamin & Grogan 2012; Frost & Epstein 2014; Myers-Smith et al. 2015; Myers-Smith & Hik 2018; Mekonnen et al. 2019; Vowles & Bjork 2019
TSP	Total summer precipitation (mm)	CRU 4.0 (Harris et al. 2014)	
TAP	Total annual precipitation (mm)	CRU 4.0 (Harris et al. 2014)	
TSR	Total summer radiation (MJ m^{-2} d^{-1})	CRU 4.0 (Harris et al. 2014)	
TAR	Total annual radiation (MJ m^{-2} d^{-1})	CRU 4.0 (Harris et al. 2014)	
Snowfall	Annual snowfall (mm)	CRU 4.0 (Harris et al. 2014)	
LOGS	Length of growing season (days)	CRU 4.0 (Harris et al. 2014)	
LOFSS	Length of full snow season (days)	MODIS-derived Snow Metrics (Lindsay et al. 2015)	
ALD	Active layer depth (m)	Geophysical Institute Permafrost Model (Luo et al. 2014)	Blok et al. 2010; Lantz et al. 2010; Lawrence & Swenson 2011; Brown et al. 2015; Huebner & Bret-Harte 2019
MASST	Mean annual soil surface temperature (°C)	Geophysical Institute Permafrost Model (Luo et al. 2014)	
MAST1m	Mean annual soil temperature at 1 m depth (°C)	Geophysical Institute Permafrost Model (Luo et al. 2014)	
Permafrost	Near-surface permafrost probability (%)	Near-surface permafrost in Alaska (Pastick et al. 2015)	Brown et al. 2015; Li et al. 2017
TPI	Topographic position index (unitless)	GMTED2010 (Danielson & Gesch 2011)	Tape et al. 2012; Tremblay et al. 2012; Frost & Epstein. 2014
Slope	Slope (degree)	GMTED2010 (Danielson & Gesch 2011)	
Aspect	Aspect (degree)	GMTED2010 (Danielson & Gesch 2011)	
Geology	Surficial geology (unitless, categorical)	Surficial Geologic of the Noatak National Preserve (Hamilton 2010)	Ackerman et al. 2017; Berner et al. 2018 Frost & Epstein. 2014
Landcover	Land cover (unitless, categorical)	NLCD Land Cover (Homer et al. 2015)	Tape et al. 2012
Fire severity	Fire severity (unitless, categorical)	MTBS archive (Eidenshink et al. 2007) and GEMI (Chen et al. 2020)	Racine et al. 2004; Mekonnen et al. 2019
PR	Proximity to nearest river/stream (m)	Computed from NHDPlus (McKay et al. 2019)	Berner et al. 2018
NP	Number of shrub patches (unitless)	Computed from our results	
SPT	Standard patch distance (m)	Computed from our results	Tape et al. 2012; Jeffers et al. 2012; Frost et al. 2013
Area	Initial area of shrub patches (m^2 ha^{-1})	Computed from our results	
Compact	Compactness of shrub patch (unitless)	Computed from our results	

TABLE 3. Detailed information of the 22 validation sites. The unburned sites were placed within the area between 500 and 2000 m radius surrounding fire perimeters.

Site No.	Tundra types	Validation fires			Geolocation	Image acquisition		
		Name	Year	Severity		Date	Resolution	Source
1	Upland	Loop Fire	1977	High	68.1° N, 161.7° W	Aug. 25, 1982 Jun. 10, 2010	0.9 m 0.6 m	Aerial Photo WorldView2
2	Upland	Loop Fire	1977	Moderate	68.0° N, 161.6° W	Aug. 25, 1982 Jun. 10, 2010	0.9 m 0.6 m	Aerial Photo WorldView2
3	Upland	Loop Fire	1977	Low	67.9° N, 161.6° W	Aug. 25, 1982 Jun. 10, 2010	0.9 m 0.6 m	Aerial Photo WorldView2
4	Upland	Loop Fire	1977	Unburned	68.0° N, 161.5° W	Aug. 25, 1982 Jun. 10, 2010	0.9 m 0.6 m	Aerial Photo WorldView2
5	Upland	Uvgoon Creek #2 Fire	1999	High	67.8° N, 162.3° W	Jul. 05, 2008 Jun. 21, 2015	1.0 m 0.5 m	IKONOS WorldView2
6	Upland	Uvgoon Creek #2 Fire	1999	Moderate	67.8° N, 162.2° W	Jul. 05, 2008 Jun. 21, 2015	1.0 m 0.5 m	IKONOS WorldView2
7	Upland	Uvgoon Creek #2 Fire	1999	Low	67.8° N, 162.2° W	Jul. 05, 2008 Jun. 21, 2015	1.0 m 0.5 m	IKONOS WorldView2
8	Upland	Uvgoon Creek #2 Fire	1999	Unburned	67.8° N, 162.1° W	Jul. 05, 2008 Jun. 21, 2015	1.0 m 0.5 m	IKONOS WorldView2
9	Lowland	Aniuk River Fire	1974	High	68.0° N, 157.9° W	Jul. 19, 1977 Jun. 30, 2010	1.5 m 0.5 m	Aerial Photo GeoEye-1
10	Lowland	Aniuk River Fire	1974	Low	68.0° N, 157.8° W	Jul. 19, 1977 Jun. 30, 2010	1.5 m 0.5 m	Aerial Photo GeoEye-1
11	Lowland	Aniuk River Fire	1974	Unburned	68.0° N, 157.9° W	Jul. 19, 1977 Jun. 30, 2010	1.5 m 0.5 m	Aerial Photo GeoEye-1
12	Lowland	Aniuk River Fire	1974	Unburned	68.0° N, 157.9° W	Jul. 19, 1977 Jun. 30, 2010	1.5 m 0.5 m	Aerial Photo GeoEye-1
13	Lowland	IAN N-110 Fire	1984	Low	68.1° N, 159.0° W	Jul. 03, 1977 Jun. 22, 2010	1.0 m 0.5 m	Declass 3 GeoEye-1
14	Lowland	IAN N-110 Fire	1984	Moderate	68.1° N, 159.0° W	Jul. 03, 1977 Jun. 22, 2010	1.0 m 0.5 m	Declass 3 GeoEye-1
15	Lowland	IAN N-110 Fire	1984	Unburned	68.1° N, 158.9° W	Jul. 03, 1977 Jun. 22, 2010	1.0 m 0.5 m	Declass 3 GeoEye-1

16	Lowland	IAN N-110 Fire	1984	Unburned	68.1° N, 159.0° W	Jul. 03, 1977 Jun. 22, 2010	1.0 m 0.5 m	Declass 3 GeoEye-1
17	Lowland	OTZ-NNW38 Fire	1977	High	67.3° N, 162.6° W	Aug. 29, 1972 Jun. 20, 2015	1.5 m 0.5 m	Aerial Photo WorldView1
18	Lowland	OTZ-NNW38 Fire	1977	Moderate	67.4° N, 162.7° W	Aug. 29, 1972 Jun. 20, 2015	1.5 m 0.5 m	Aerial Photo WorldView1
19	Lowland	OTZ-NNW38 Fire	1977	Low	67.5° N, 162.6° W	Aug. 29, 1972 Jun. 20, 2015	1.5 m 0.5 m	Aerial Photo WorldView1
20	Lowland	OTZ-NNW38 Fire	1977	Unburned	67.5° N, 162.6° W	Aug. 29, 1972 Jun. 20, 2015	1.5 m 0.5 m	Aerial Photo WorldView1
21	Lowland	OTZ-NNW38 Fire	1977	Unburned	67.5° N, 162.4° W	Aug. 29, 1972 Jun. 20, 2015	1.5 m 0.5 m	Aerial Photo WorldView1
22	Lowland	OTZ-NNW38 Fire	1977	Unburned	67.3° N, 162.9° W	Aug. 29, 1972 Jun. 20, 2015	1.5 m 0.5 m	Aerial Photo WorldView1

Figure legends

FIGURE 1. Tundra fires selected for studying decadal patterns of shrub-cover change in the Noatak National Preserve. The maps plotted refer to the 1977 OTZ-NNW38 Fire (a), the 1986 OTZ-NE100 Fire (b), the 1976 S-Noatak Fire (c) and the 1982 IAN-NE25 Fire (d) in the Noatak National Preserve (e). All study sites (white circles, n = 114, 250 × 250 m) and validation sites (green circles, n = 22, 250 × 250 m) were randomly selected across burned and unburned upland and lowland tundra. The unburned zone is defined as the region beyond 500 m and within 2000 m radius surrounding the fire perimeter, and the transition zone refers to the area between burned and unburned zone. The historical fire perimeters were acquired from the Alaska Interagency Coordination Center (AICC 1950-2020). Fire severity maps referred to Chen et al. (2020) and Monitoring Trends in Burn Severity (MTBS 1984-2020). The geospatial data were superimposed on the GMTED2010 global elevation dataset (Danielson & Gesch 2011).

FIGURE 2. Time series of shrub-cover dynamics in upland and lowland tundra. The red dotted lines indicate the year of fire occurrence. Negative values on the *x* axis (years since fire) represent the number of years before fire occurrence, while positive values indicate years after fire. All data are shown in mean ± 1 SE.

FIGURE 3. Example of decadal patterns of shrub-cover change in burned and unburned upland tundra. The high resolution (1.0 m) aerial and satellite images (1st column) and the associated shrub-cover maps (2nd column) were displayed sequentially over time. The fire severity map was obtained from MTBS (1984-2020).

FIGURE 4. Example of decadal patterns of shrub-cover change in burned and unburned lowland tundra. The high resolution (1.0 m) aerial and satellite images (1st column) and the associated shrub-cover maps (2nd column) were displayed sequentially over time. The fire severity map was obtained from Chen et al. (2020).

FIGURE 5. Multivariate regression models for shrub-cover change in upland and lowland tundra. The mean linear regression trendline is bounded by 95% confidence interval. The inserted pie charts show the relative contribution of each variable retained in the model to overall variance. Variables in red and blue represent positive and negative correlation with shrub-cover change, respectively. TSP: total summer precipitation (mm); Area: initial shrub area (m^2 ha^{-1}); MSAT: mean summer air temperature (^oC); Permafrost: permafrost probability (%); and LOGS: length of growing season (days).

FIGURE 6. Conceptual models demonstrating the interactions between climate change, fire disturbance, and shrub-cover dynamics in upland and lowland tundra ecosystems. '+' and '–' symbols represent positive and negative feedbacks, respectively. Dark red lines represent feedbacks in burned tundra, and dark green lines are for unburned tundra. Black lines are feedbacks applied to both burned and unburned tundra.

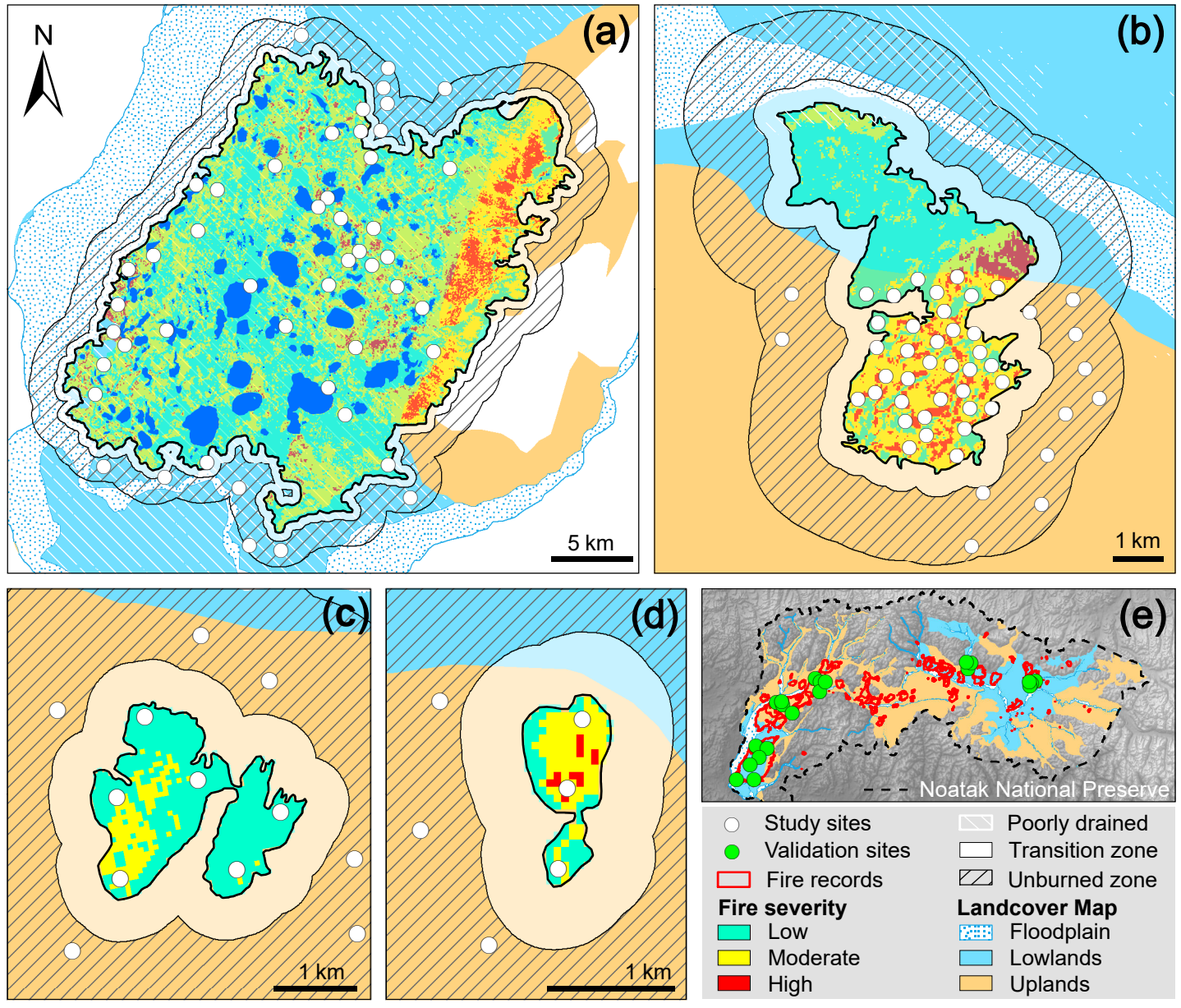
N
(a)
5 km
(b)
1 km
(c)
1 km
(d)
1 km
(e)
Noatak National Preserve
Study sites
Validation sites
Fire records
Fire severity
Low
Moderate
High
Poorly drained
Transition zone
Unburned zone
Landcover Map
Floodplain
Lowlands
Uplands

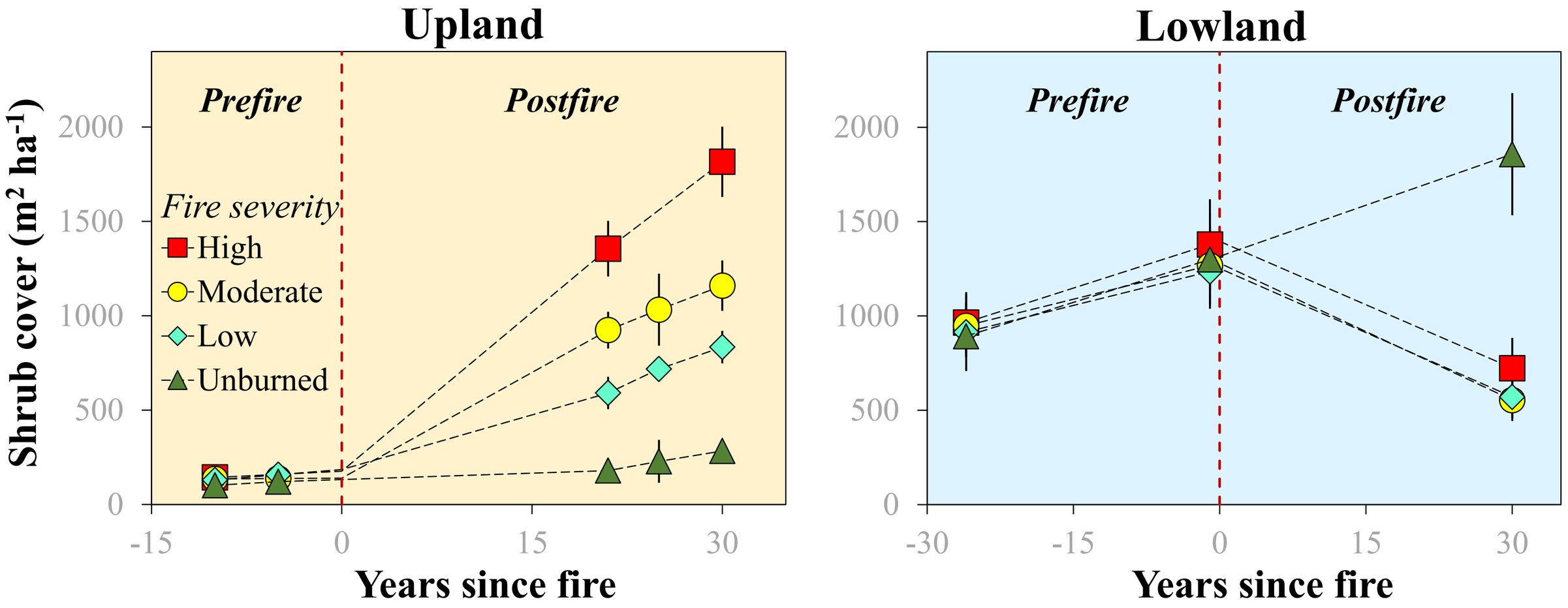
Upland
Lowland
Prefire
Postfire
Fire severity
High
Moderate
Low
Unburned
Shrub cover (m² ha⁻¹)
Years since fire
0
500
1000
1500
2000
-30
-15
0
15
30

Imagery

Shrub cover

1977

1986

2007

2016

Year

Fire Severity Map

Moderate

Low

Unburned

N

W

E

S

0 125 250 500

m

Shrub cover

Imagery

Shrub cover

1951

1976

1977

1984

2015

Year

Fire Severity Map

Moderate

Low

Unburned

N

W

E

S

0 100 200 400

m

Shrub cover

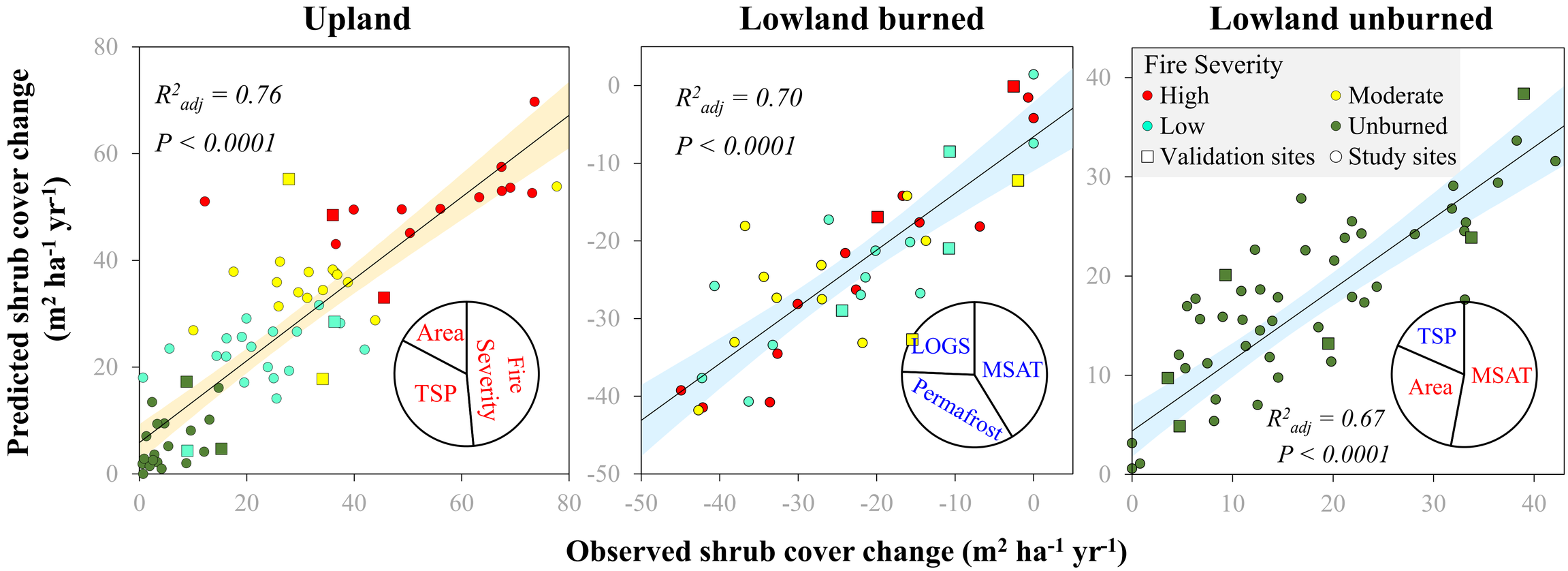
Upland
Lowland burned
Lowland unburned
Predicted shrub cover change (m² ha⁻¹ yr⁻¹)
Observed shrub cover change (m² ha⁻¹ yr⁻¹)
R²adj = 0.76
P < 0.0001
R²adj = 0.70
P < 0.0001
R²adj = 0.67
P < 0.0001
Area
Fire Severity
TSP
LOGS
MSAT
Permafrost
TSP
Area
MSAT
Fire Severity
High
Moderate
Low
Unburned
Validation sites
Study sites
0
20
40
60
80
-50
-40
-30
-20
-10
0
10
20
30
40

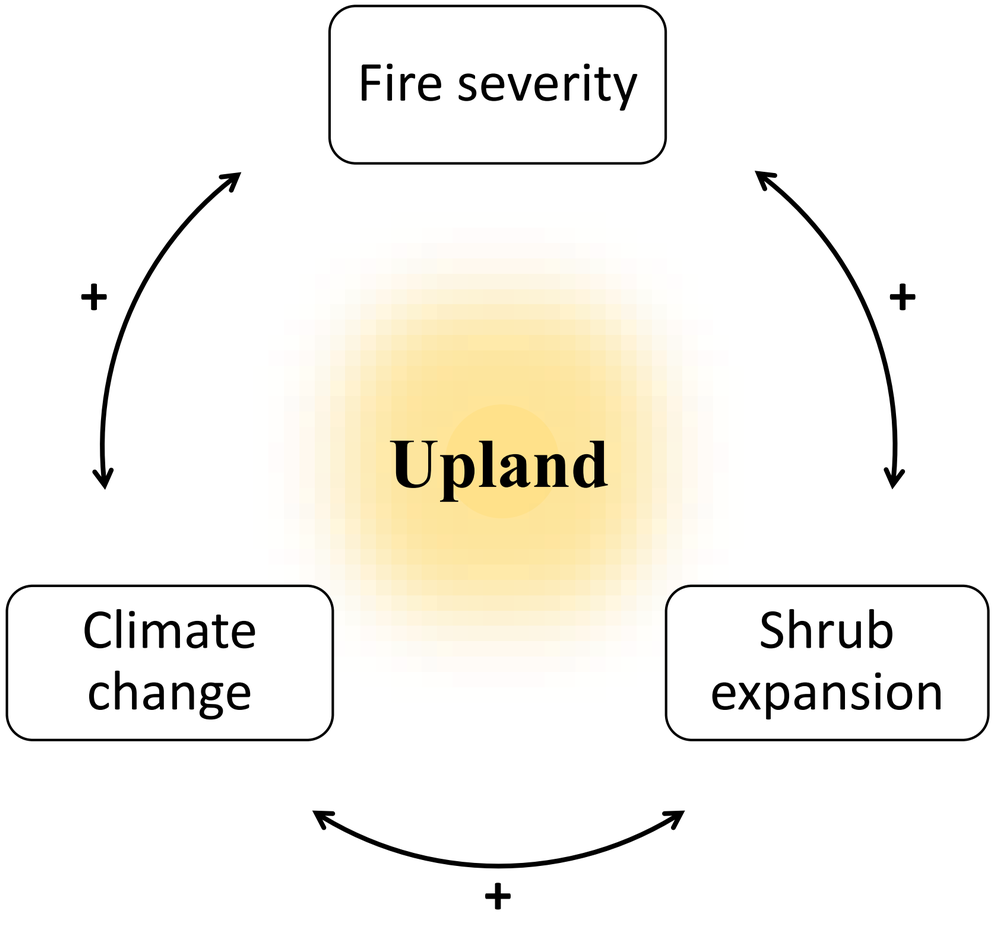
Fire severity
Upland
Climate change
Shrub expansion
+
+
+

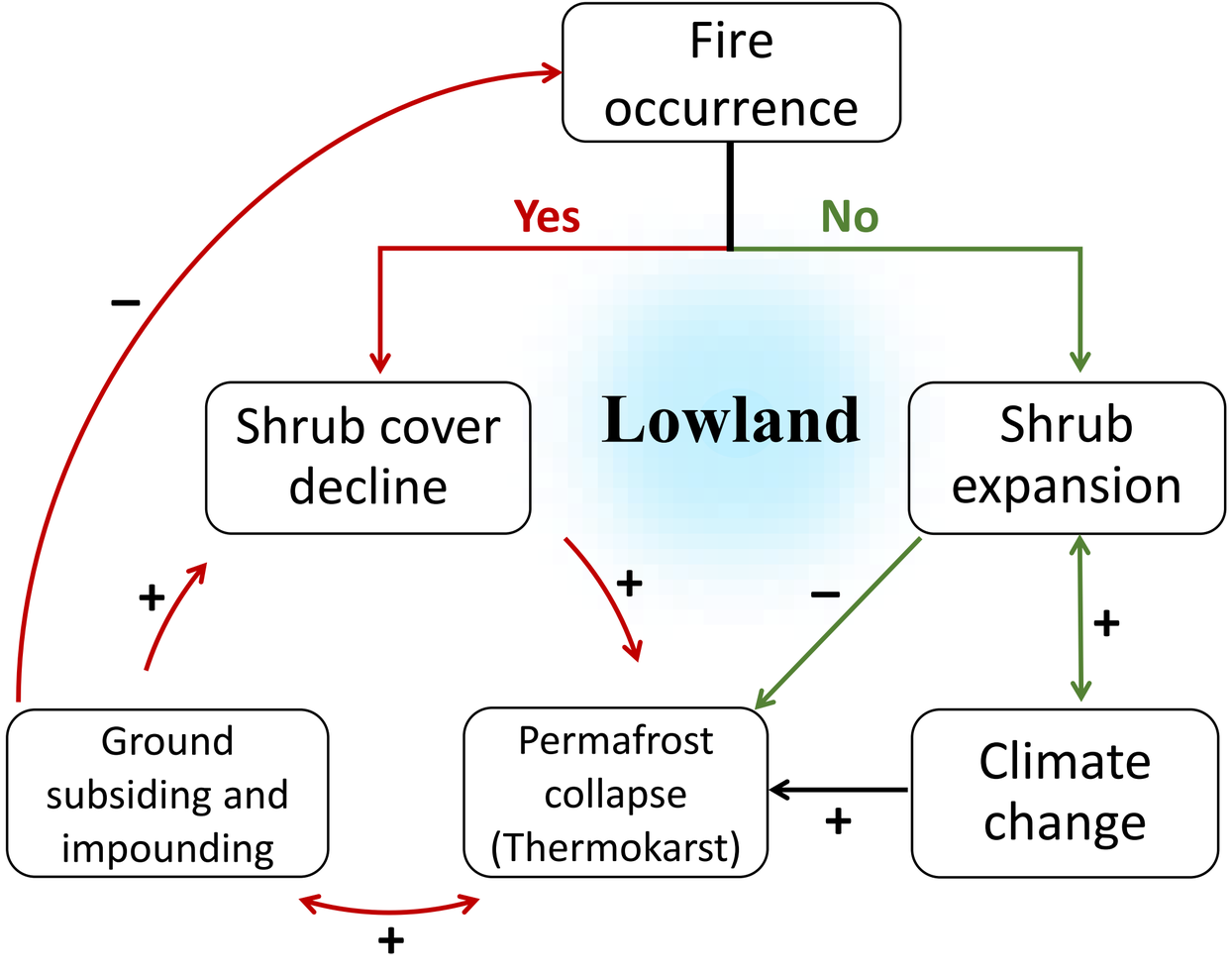
Fire occurrence
Yes
No
Shrub cover decline
Lowland
Shrub expansion
Ground subsiding and impounding
Permafrost collapse (Thermokarst)
Climate change
−
+
+
−
+
+
+